International Journal of Mass Spectrometry 293 (2010) 28–33

Contents lists available at ScienceDirect

International Journal of Mass Spectrometry

journal homepage: www.elsevier.com/locate/ijms

Determination of absolute photoionization cross-sections of oxygenated hydrocarbons

Mingfeng Xie, Zhongyue Zhou, Zhandong Wang, Dongna Chen, Fei Qi*

National Synchrotron Radiation Laboratory, University of Science and Technology of China, Hefei, Anhui 230029, PR China

ARTICLE INFO

Article history:
Received 7 February 2010
Received in revised form 22 March 2010
Accepted 23 March 2010
Available online 30 March 2010

Keywords:
Absolute photoionization cross-section
Oxygenated hydrocarbon
VUV photoionization
Mass spectrometry

ABSTRACT

The near-threshold absolute photoionization cross-sections of 12 oxygenated hydrocarbons, including 1-butanol, 2-butanol, *iso*-butanol, *tert*-butanol, 1-pentanol, *tert*-pentanol, *iso*-pentanol, methyl *tert*-butyl ether (MTBE), ethyl *tert*-butyl ether (ETBE), furan, 2-methylfuran, 2,5-dimethylfuran, were measured in the photon energy range from respective ionization thresholds to 11.5 eV. The experiments were performed with photoionization mass spectrometry and tunable synchrotron vacuum ultraviolet (VUV) light. Binary-liquid-mixtures of the investigated sample and benzene were used in the measurements where benzene acts as a calibration standard, due to its well known photoionization cross-section at the photon energies from its ionization energy (9.24 eV) to 11.5 eV. Photodissociative fragments from the molecules were also observed, and their photodissociation cross-sections are also presented.

1. Introduction

There is a considerable recent interest in the development of alternative fuels to reduce excessive consumption of fossil fuels [1]. Among the most important alternative fuels are renewable oxygenated biofuels, including vegetable oil, biodiesel, bioalcohols, bioethers, biogas, etc. Many groups have carried out experiments by mass spectrometry (MS) with gas or liquid chromatography [2–4]. Photoionization mass spectrometry is also widely used with the benefits of producing less fragmentation than conventional electron-impact ionization [5–7]. However, quantitative analysis is always difficult in the absence of photoionization cross-section data of these biofuels and their reaction intermediates. Several methods have been developed for the determination of photoionization cross-sections. The double ion chamber method was used by Samson et al. to measure the photoionization cross-sections of inert gases and water [8,9]. West and Kjeldsen used the merged-beam method for measurement of photoionization cross-sections of atomic ions [10,11]. For molecules, Cool et al. developed the photoionization mass spectrometry (PIMS) method with synchrotron VUV radiation for determining total and partial photoionization cross-sections of hydrocarbons and oxygenated hydrocarbons using binary gas mixtures of the standard (propene) and target species [12,13]. Neumark et al. used photofragment translational spectroscopy combined with synchrotron VUV photoionization to determine the photoionization cross-sections of some free radicals [14–16].

Using the methods mentioned above, the photonization cross-sections of some biofuels have been obtained by different groups. Kamel et al. determined relative photoionization cross-section curves for molecular and fragment ions of methanol, ethanol, *n*-propanol and *iso*-propanol from their ionization potentials to 14.0 eV using the PIMS method [17]. In the 1970s, Person and Nicole studied the isotope effects in the cross-sections for methanol and ethanol with a dual beam single ion chamber technique [18]. Later in the 1980s, synchrotron radiation began to be used for the determination of cross-sections of methyl, ethyl and propyl alcohols by Hatano et al. [19] More recently, Adam and Zimmermann measured the cross-sections of ethanol, propanol and ethers at 118 nm using laser-based single-photon ionization time-of-flight mass spectrometer (SPI-TOFMS) [20]. Cool et al. measured C1–C3 alcohols, dimethyl ether (DME), methyl acetate, ethyl acetate and tetrahydrofuran using the PIMS method with synchrotron VUV light [12].

In this paper, we use the synchrotron VUV PIMS method to determine the absolute photoionization cross-section using binary-liquid-mixtures of the standard and target molecular. Here, we present absolute photoionization cross-sections of 12 oxygenated hydrocarbons, including C4–C5 alcohols, MTBE, ETBE, furan, 2-methylfuran and 2,5-dimethylfuran. Cross-sections for dissociative fragments are also presented for these molecules.

2. Experimental

2.1. Instrumentation

The experiments were carried out at the National Synchrotron Radiation Laboratory (NSRL) in Hefei, China. The beamline and

* Corresponding author. Tel.: +86 551 3602125; fax: +86 551 5141078.
E-mail address: fqi@ustc.edu.cn (F. Qi).

1387-3806/$ – see front matter © 2010 Elsevier B.V. All rights reserved.
doi:10.1016/j.ijms.2010.03.007

the experimental apparatus were reported in our previous reports [21,22]. In brief, synchrotron radiation from a bending magnet beamline was dispersed by a 1 m Seya-Namioka monochromator (home-made) equipped with a grating coated with Au (1200 grooves/mm). The energy resolution ($E/\Delta E$) is about 500. A 0.5 mm thick LiF filter was used to eliminate higher-order harmonic radiation at photon energies below 11.7 eV.

The experimental setup consists of a source chamber with a gas feeding system, a differentially pumped chamber and a photoionization chamber with a home-made reflection time-of-flight (RTOF) mass spectrometer. The sampled species formed a molecular beam through a quartz nozzle with a 0.3 mm diameter orifice and a nickel skimmer with a 1.25 mm diameter aperture, and passed into the photoionization chamber, where the molecular beam was intersected and ionized by the tunable VUV light. Photoions were propelled into the flight tube by a pulse extraction field triggered by a DG 535 pulse generator (Stanford Research Systems, Inc. Sunnyvale, CA, USA), and then ions were reflected to a microchannel plate (MCP) detector. After amplification by a VT120C preamplifier (EG & G, ORTEC, Oak Ridge, TN, USA), the ion signal was recorded by a P7888 multiscaler (FAST Comtec, Oberhaching, Germany). A silicon photodiode SXUV-100 (International Radiation Detectors Inc., CA, USA) was used to monitor the photon flux for normalizing the ion signals after quantum efficiency corrections to the photodiode response.

2.2. Measurement procedure

The binary-liquid-mixture method was applied in the measurements [21]. The absolute photoionization cross-sections of benzene measured by Rennie et al. [23] were used as the calibration standard. When the mole ratio of target to standard molecules in the binary mixture equals one, the ratio of target to standard ion signal can be expressed by the equation [12,21],

$$\frac{S_T}{S_S} = \left[\frac{\sigma_T(E)}{\sigma_S(E)}\right]\left[\frac{R_T}{R_S}\right] \quad (1)$$

Here the subscript T and S denote the target and standard molecules. $\sigma(E)$ is the photoionization cross-section at the photon energy of E; R is a mass-dependent response factor that accounts for different sampling and detection efficiencies, which was reported in our previous work [21]. S is the integrated signal-intensity, which has been normalized by the photon flux and plotted as a function of the photon energy, yielding the photoionization efficiency (PIE) spectra. Over the energy range from 9.24 eV (the IE of benzene) to 11.5 eV, the absolute photoionization cross-sections of target molecules were obtained by Eq. (1). For species with IEs lower than 9.24 eV, the absolute photoionization cross-sections were obtained by extrapolating their PIE curves to the ionization thresholds. Corrections for interference from overlapping signals from isotopomers were included in the calculation process discussed above.

Binary mixtures of benzene and target species at the mole ratio of 1:1 were pumped into the vaporizer with the flow rate controlled by a high performance liquid chromatograph pump (Fuli Analytical Instrument Co., Ltd., Zhejiang, China). The vaporized mixture was then diluted by argon, the flow rate of which was kept at 0.25 SLM (standard liters per minute) by a MKS mass flow controller. Subsequently, the gas consisting of 5% vaporized mixture and 95% argon was fed into the source chamber through a stainless steel tube, which was heated to avoid condensation. The distance between the exit of the stainless steel tube and the sampling quartz nozzle was 10 mm. The pressure of the source chamber was kept at 5 Torr, controlled by a MKS throttle valve (MKS Instruments, Andover, MA, USA).

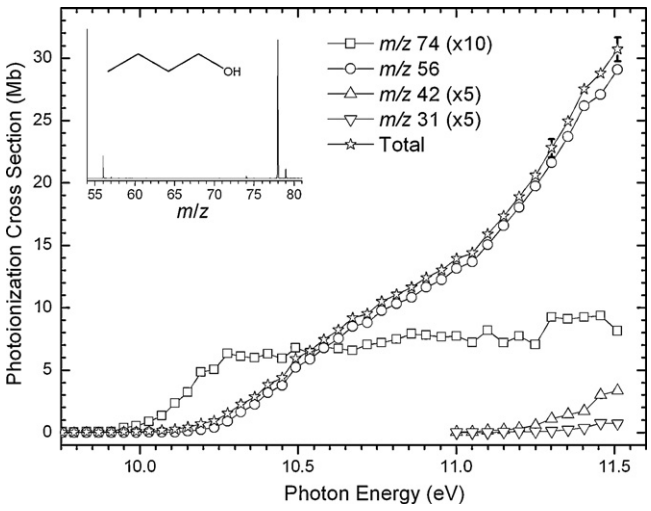

Fig. 1. Absolute photoionization cross-sections of 1-butanol. The error bars denote standard deviations of four replicates with separately prepared binary mixtures. The inserted photoionization mass spectra in this and other figures were measured at the photon energy of 10.5 eV.

1-Butanol (99%), 2-butanol (CP), *iso*-butanol (97+%), *tert*-butanol (98+%), 1-pentanol (98.5+%), *tert*-pentanol (CP), *iso*-pentanol (98.5%) and furan (CP) were purchased from Sinopharm Chemical Reagent Co., Ltd. (Shanghai, China). MTBE (99%) and ETBE (95+%) were purchased from TCI (Shanghai) Development Co., Ltd. (Shanghai, China). 2-Methylfuran (98+%) and 2,5-dimethylfuran (99%) were purchased from Aladdin Reagent Database Inc. (Shanghai, China). All chemicals were used without further purification.

3. Results

Figs. 1–12 show the measured photoionization cross-sections of 12 oxygenated hydrocarbons in this work. The inserted plots in the figures are partial photoionization mass spectra measured at the photon energy of 10.5 eV. The error bars in the figures are standard deviations of separate measurements with separately prepared binary mixtures. For most compounds, the standard deviations for the measurements are about ±5%. The uncertainty of benzene cross-sections is probably about ±15%. Besides, considering the errors of mass discrimination factors by ±15% and the purity of chemicals, a reasonable uncertainty of tabulated cross-sections about ±25% is estimated in present work. The tabulated data are provided as the supplementary material of this paper. The detailed description on the investigated molecules is provided below.

3.1. 1-Butanol, iso-butanol, 2-butanol and tert-butanol

Figs. 1–4 display the absolute photoionization cross-sections of 1-butanol, *iso*-butanol, 2-butanol and *tert*-butanol in the photon energy range from their respective IEs to 11.5 eV. As shown in Fig. 1, the photoionization cross-section of 1-C_4H_9OH (m/z 74) rises slowly from the ionization threshold to a plateau near 10.25 eV. The IE of 1-butanol is 9.95 ± 0.05 eV, which is in good agreement with the reference value (9.99 ± 0.05) in NIST online database [24]. The main photodissociation fragment observed in this work is $C_4H_8^+$ (m/z 56), its appearance energy is 10.19 ± 0.05 eV, which agrees well with the literature value (10.20 ± 0.10 eV) measured using the electron-impact method [25]. $C_2H_2O^+$ (m/z 42) and CH_3O^+ (m/z 31) were also observed as photodissociation fragments in this study, but only contribute slightly to the total photoionization cross-section. The appearance energies of $C_2H_2O^+$ and CH_3O^+ are 11.10 and 11.30 ± 0.05 eV, respectively, both of which agree

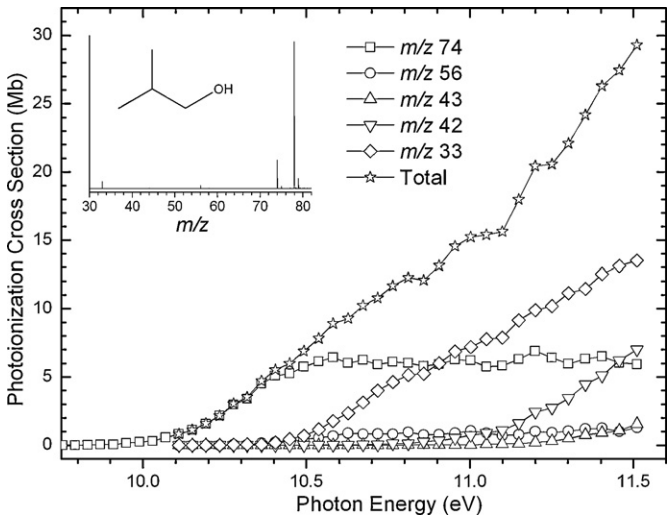

Fig. 2. Absolute photoionization cross-sections of *iso*-butanol.

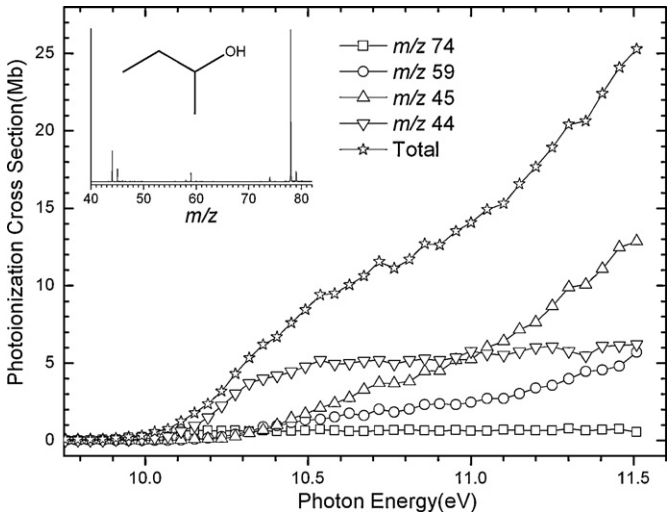

Fig. 3. Absolute photoionization cross-sections of 2-butanol.

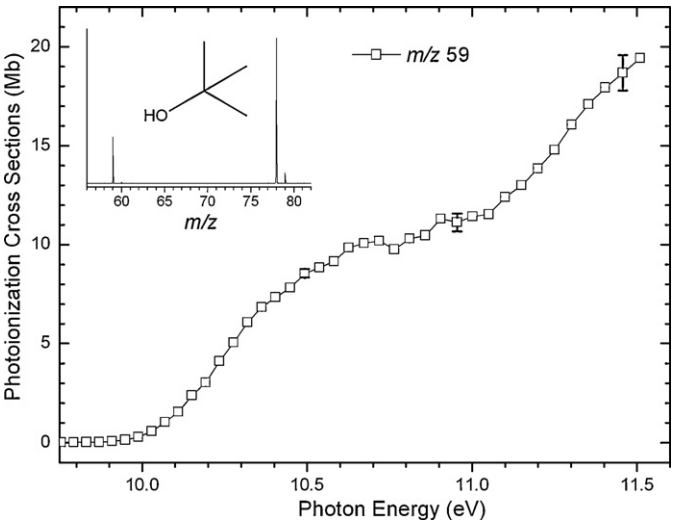

Fig. 4. Absolute photoionization cross-sections of *tert*-butanol. The error bars denote standard deviations of two replicates with separately prepared binary mixtures.

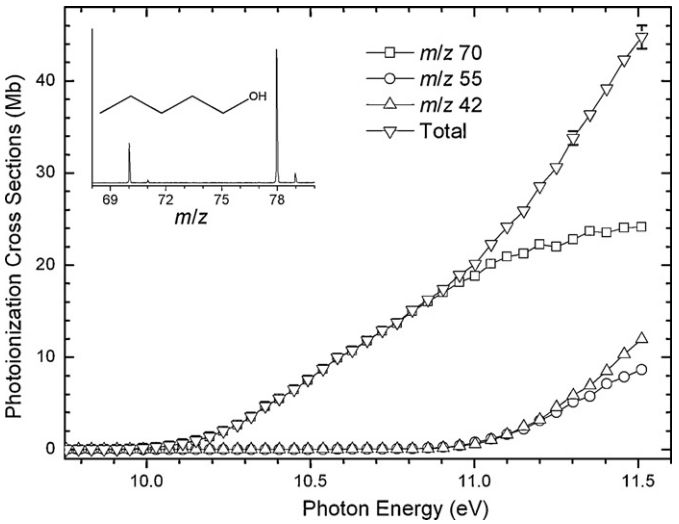

Fig. 5. Absolute photoionization cross-sections of 1-pentanol. The error bars denote standard deviations of two replicates with separately prepared binary mixtures.

with the literature values within the measurement uncertainties [26,27].

For *iso*-butanol (Fig. 2), the IE (9.95 ± 0.05 eV) measured in this work agrees well with the reference value (10.02 ± 0.02 eV) [24]. Four photodissociation fragments, $C_4H_8^+$ (m/z 56), $C_3H_7^+$ (m/z 43), $C_3H_6^+$ (m/z 42) and CH_5O^+ (m/z 33), were observed in this work. The fragment CH_5O^+ is a major photodissociation product, with an appearance energy of 10.36 ± 0.05 eV, which is 0.07 eV lower than that obtained using the PIPECO method [28]. The appearance energy of the fragment $C_3H_6^+$ is 10.81 ± 0.05 eV in this work, which is also lower than reference value (11.00 ± 0.03 eV) [28]. The other two fragments $C_4H_8^+$ and $C_3H_7^+$ make minor contribution to the total photoionization cross-section, with the appearance energies of 10.32 and 11.00 ± 0.05 eV, respectively.

For 2-butanol, as shown in Fig. 3, the molecular ion $C_4H_9OH^+$ (m/z 74) makes a little contribution to the total photoionization cross-section. The IE of 9.87 ± 0.03 eV observed in this work is in excellent agreement with the reference value (9.88 ± 0.03 eV) [24]. The prominent photodissociation fragments observed are $C_3H_7O^+$ (m/z 59), $C_2H_5O^+$ (m/z 45) and $C_2H_4O^+$ (m/z 44), with appearance energies of 10.19, 10.11 and 9.91 ± 0.05 eV, respectively; all of them agree with the literature values within the error range [25,28]. The fragment $C_3H_6O^+$ (m/z 58) (not shown in Fig. 3, see the supplementary material) was also observed above 10.22 eV but contributes only slightly to the total photoionization cross-section. The $C_3H_8O^+$ (m/z 60) ion was reported with an appearance energy (AE) of 10.22 eV using the electron-impact method [25], but was not observed in our work.

For *tert*-butanol, the molecular ion $C_4H_9OH^+$ (m/z 74) was not observed in this work. The only fragment is $C_3H_7O^+$ (m/z 59), and the appearance energy is 9.87 ± 0.03 eV, which is identical to that obtained using the photoionization method reported in the literature [29]. To our knowledge, no previous measurements of the absolute photoionization cross-sections of these four isomeric butanols have been reported.

3.2. 1-Pentanol, iso-pentanol and tert-pentanol

The photodissociation cross-sections of 1-pentanol are presented in Fig. 5. The molecular ion $C_5H_{12}O^+$ (m/z 88) was not observed in this work. The major fragment is $C_5H_{10}^+$ (m/z 70), indicating that the C–O bond cleavage is dominant. The appearance energy of $C_5H_{10}^+$ is 9.95 ± 0.05 eV, which is a little lower than the lit-

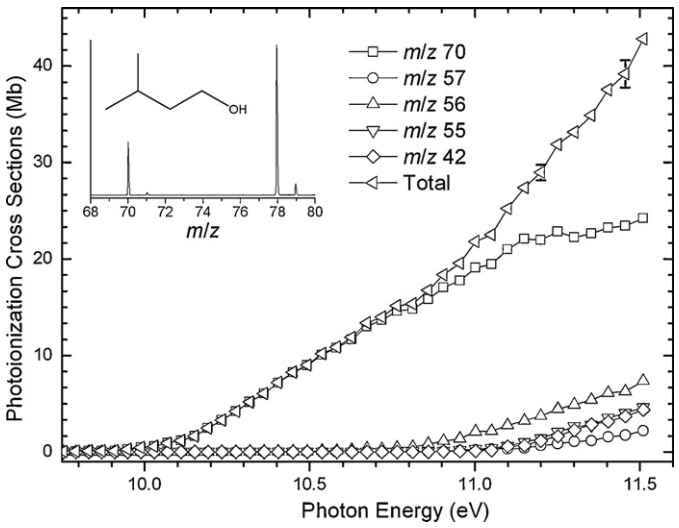

Fig. 6. Absolute photoionization cross-sections of *iso*-pentanol. The error bars denote standard deviations of two replicates with separately prepared binary mixtures.

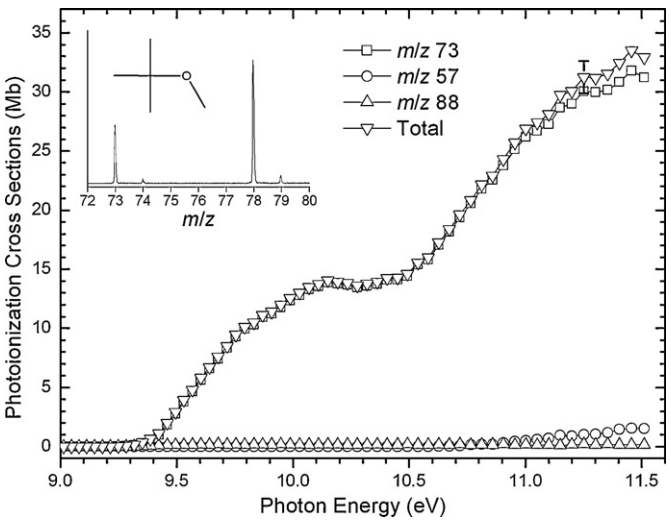

Fig. 8. Absolute photoionization cross-sections of MTBE. The error bars denote standard deviations of three replicates with separately prepared binary mixtures.

erature value (10.04 ± 0.05 eV) [30]. The fragments m/z 55 ($C_4H_7^+$) and m/z 42 ($C_3H_6^+$) were also observed above 10.86 eV.

As shown in Fig. 6, the situation of photoionization of *iso*-pentanol is quite similar to that of 1-pentanol. From its IE around 10 eV, the total photoionization cross-sections increase mainly due to the fragment ion $C_5H_{10}^+/C_4H_6O^+$ (m/z 70) below ~10.9 eV and then rise a little faster with appearances of fragment ions at m/z 57 ($C_4H_9^+/C_3H_5O^+$), 56 ($C_4H_8^+/C_3H_4O^+$), 55 ($C_4H_7^+/C_3H_3O^+$) and 42 ($C_3H_6^+/C_2H_2O^+$) above ~10.9 eV. The molecular ion is unstable and thus was not detected.

For *tert*-pentanol (in Fig. 7), the total photoionization cross-section is attributed to the major fragments $C_4H_9O^+$ (m/z 73) and $C_3H_7O^+$ (m/z 59), with appearance energies at 9.89 and 9.80 eV, respectively. The uncertainties for the photoionization cross-section measurement of 1-pentanol, *iso*-pentanol and *tert*-pentanol are below 25%.

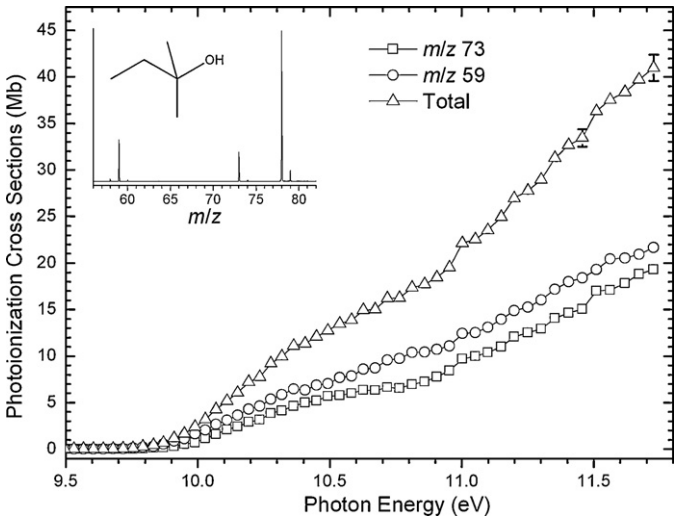

Fig. 7. Absolute photoionization cross-sections of *tert*-pentanol. The error bars denote standard deviations of two replicates with separately prepared binary mixtures.

3.3. MTBE and ETBE

MTBE is commonly used as a gasoline additive to reduce emissions of CO, O_3, C_6H_6, etc. [31] and raise the octane number of gasoline [32]. However, its use has declined in several countries, including the USA, since MTBE contaminants the environment and is harmful to the human body. ETBE is a cleaner additive used as a gasoline octane booster of possible benefit for replacement of MTBE [33,34].

Figs. 8 and 9 present the photoionization cross-sections of MTBE and ETBE, respectively. For MTBE, the major photodissociation product is $C_4H_9O^+$ (m/z 73) with the appearance energy of 9.25 ± 0.03 eV, which is lower than the literature value (9.46 eV) obtained using the electron-impact method [35]. The fragment $C_4H_9^+$ (m/z 57) was also observed above 10.49 eV, but contributes only slightly to the total photoionization cross-section. For ETBE, as shown in Fig. 9, the parent molecular ion is not observed. Four photodissociation fragments, $C_5H_{11}O^+$ (m/z 87), $C_3H_7O^+$ (m/z 59), $C_4H_9^+$ (m/z 57) and $C_4H_8^+$ (m/z 56), were observed in this work. The fragment $C_5H_{11}O^+$ appears at 9.11 ± 0.03 eV, about 0.1 eV lower than the literature value [36]. The other three fragments appear

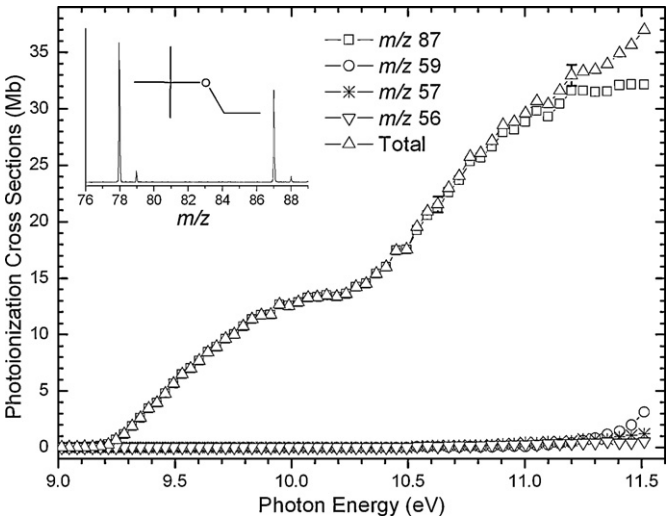

Fig. 9. Absolute photoionization cross-sections of ETBE. The error bars denote standard deviations of two replicates with separately prepared binary mixtures.

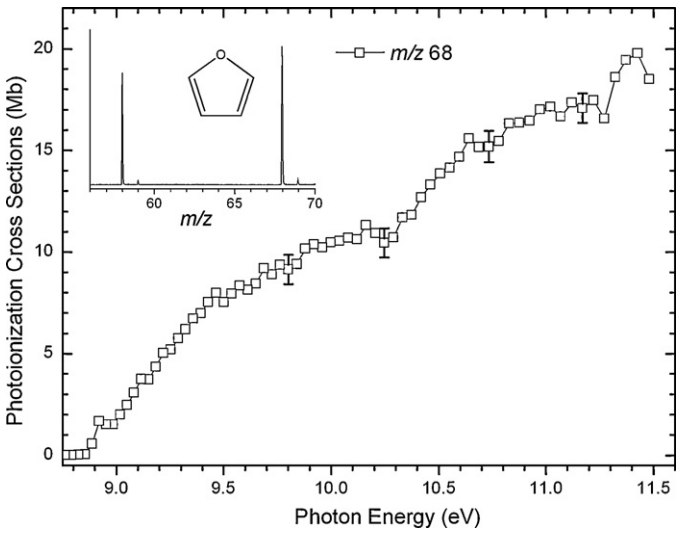

Fig. 10. Absolute photoionization cross-sections of furan. The error bars denote standard deviations of three replicates with separately prepared binary mixtures.

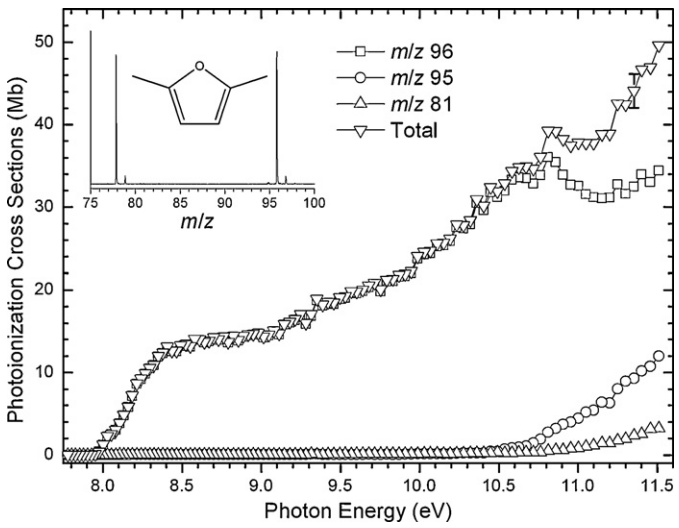

Fig. 12. Absolute photoionization cross-sections of 2,5-dimethylfuran. The error bars denote standard deviations of two replicates with separately prepared binary mixtures.

near 10.5 eV, but make little contributions to the total photoionization cross-section. To our knowledge, no previous measurements on photoionization cross-sections of these two ethers are reported.

3.4. Furan, 2-methylfuran and 2,5-dimethylfuran

Fig. 10 shows the absolute photoionization cross-section of furan. Due to the low solubility of furan in benzene, acetone was chosen as the calibration standard for the measurement of photoionization cross-sections of furan. The absolute photoionization cross-sections of acetone have been measured by Cool et al. [12]. using propene as the calibration standard, which are in good agreement with the result reported by Person and Nicole [37]. We have also measured the absolute photoionization cross-sections of acetone using benzene as the calibration standard [21], in good agreement with the data of Cool et al. As shown in Fig. 10, only the molecular ion of $C_4H_4O^+$ (m/z 68) was observed in this work. The IE is 8.86 ± 0.03 eV, which is in good agreement with the literature value (8.88 ± 0.01 eV) [24]. The appearance energy of the photodissociation fragment $C_3H_4^+$ (m/z 40) is 11.48 ± 0.05 eV (EI) [38] or 12.7 ± 0.1 eV (CEMS) [39], but it was not observed in this work. To our knowledge, no previous reports of photoionization cross-sections of furan are available.

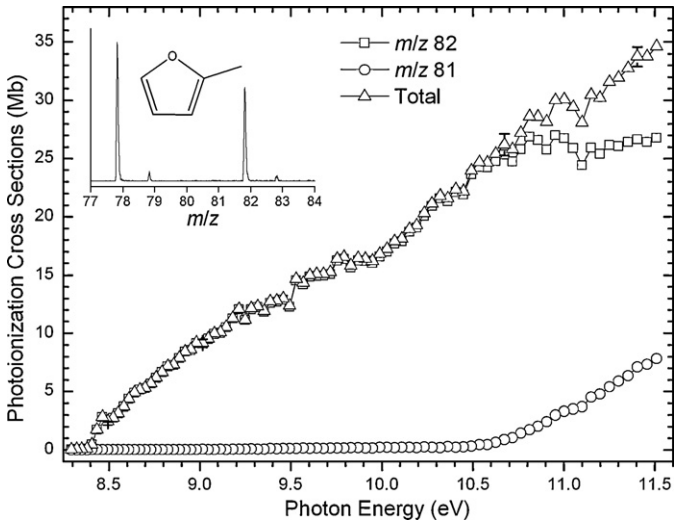

Fig. 11. Absolute photoionization cross-sections of 2-methylfuran. The error bars denote standard deviations of four replicates with separately prepared binary mixtures.

Figs. 11 and 12 show the absolute photoionization and photodissociation cross-sections of 2-methylfuran and 2,5-dimethylfuran. Benzene was used as calibration standard for these two methyl-substituted furans for both of them show good solubility with benzene. The IE of 2-methylfuran is 8.38 ± 0.03 eV, which is identical to the literature value [24]. The fragment $C_5H_5O^+$ (m/z 81) was also observed above 10.54 eV, but makes little contribution to the total cross-sections.

For 2,5-dimethylfuran, the IE is 7.95 ± 0.03 eV, which agrees with the data of the NIST online database (7.8–8.03 eV). The two photodissociation fragments $C_6H_7O^+$ (m/z 95) and $C_5H_5O^+$ (m/z 81) appear at 10.45 and 10.76 eV, respectively, but the fragment $C_5H_5O^+$ makes little contribution to the total photoionization cross-section. To our knowledge, no previous measurements on photoionization cross-sections of the two methyl-substituted furans have been reported.

4. Conclusion

Experimental determinations of absolute photoionization cross-sections of 12 oxygenated biofuels were performed over the energy range of 8.0–11.5 eV with tunable synchrotron VUV photoionization and molecular-beam mass spectrometry. All of these data are useful for quantitative analysis of organic compounds involving photoionization. They are especially important for calculating the concentrations of combustion intermediates, which are essential for kinetic modeling studies of relevant combustion chemistry. The binary-liquid-mixture method used in this experiment has been proved to be feasible and reliable for species that can form solution. But the method is limited when extended to determine the photoionization cross-sections of solid compounds with higher boiling points and lower stability.

Supporting information

Tabulated photoionization cross-sections for the species measured in the present work are available in the online version of this article.

Acknowledgements

This work was supported by Chinese Academy of Sciences, Natural Science Foundation of China (50925623 and 10805047), and Ministry of Science and Technology of China (2007CB815204 and 2007DFA61310).

Appendix A. Supplementary data

Supplementary data associated with this article can be found, in the online version, at doi:10.1016/j.ijms.2010.03.007.

References

[1] T.V. Ramachandra, N.V. Joshi, D.K. Subramanian, Renew. Sust. Energ. Rev. 4 (2000) 375.
[2] K.M. Doll, B.K. Sharma, P.A.Z. Suarez, S.Z. Erhan, Energy Fuels 22 (2008) 2061.
[3] P.A.Z. Suarez, B.R. Moser, B.K. Sharma, S.Z. Erhan, Fuel 88 (2009) 1143.
[4] S.P. Zou, Y.L. Wu, M.D. Yang, C. Li, J.M. Tong, Energy Fuels 23 (2009) 3753.
[5] Y.Y. Li, L.X. Wei, Z.Y. Tian, B. Yang, J. Wang, T.C. Zhang, F. Qi, Combust. Flame 152 (2008) 336.
[6] X.S. Wu, Z.H. Huang, T. Yuan, K.W. Zhang, L.X. Wei, Combust. Flame 156 (2009) 1365.
[7] T.C. Zhang, J. Wang, T. Yuan, X. Hong, L.D. Zhang, F. Qi, J. Phys. Chem. A 112 (2008) 10487.
[8] G.N. Haddad, J.A.R. Samson, J. Chem. Phys. 84 (1986) 6623.
[9] J.A.R. Samson, W.C. Stolte, J. Electron. Spectrosc. Relat. Phenom. 123 (2002) 265.
[10] H. Kjeldsen, J. Phys. B: At. Mol. Opt. Phys. 39 (2006) R325.
[11] J.B. West, J. Phys. B: At. Mol. Opt. Phys. 34 (2001) R45.
[12] T.A. Cool, J. Wang, K. Nakajima, C.A. Taatjes, Int. J. Mass Spectrom. 247 (2005) 18.
[13] J. Wang, B. Yang, T.A. Cool, N. Hansen, T. Kasper, Int. J. Mass Spectrom. 269 (2008) 210.
[14] J.C. Robinson, N.E. Sveum, D.M. Neumark, J. Chem. Phys. 119 (2003) 5311.
[15] J.C. Robinson, N.E. Sveum, D.M. Neumark, Chem. Phys. Lett. 383 (2004) 601.
[16] N.E. Sveum, S.J. Goncher, D.M. Neumark, Phys. Chem. Chem. Phys. 8 (2006) 592.
[17] K.M.A. Refaey, W.A. Chupka, J. Chem. Phys. 48 (1968) 5205.
[18] J.C. Person, P.P. Nicole, J. Chem. Phys. 55 (1971) 3390.
[19] H. Koizumi, K. Hironaka, K. Shinsaka, S. Arai, H. Nakazawa, A. Kimura, Y. Hatano, Y. Ito, Y. Zhang, A. Yagishita, K. Ito, K. Tanaka, J. Chem. Phys. 85 (1986) 4276.
[20] T. Adam, R. Zimmermann, Anal. Bioanal. Chem. 389 (2007) 1941.
[21] Z.Y. Zhou, M.F. Xie, Z.D. Wang, F. Qi, Rapid Commun. Mass Spectrom. 23 (2009) 3994.
[22] F. Qi, R. Yang, B. Yang, C.Q. Huang, L.X. Wei, J. Wang, L.S. Sheng, Y.W. Zhang, Rev. Sci. Instrum. 77 (2006) 084101.
[23] E.E. Rennie, C.A.F. Johnson, J.E. Parker, D.M.P. Holland, D.A. Shaw, M.A. Hayes, Chem. Phys. 229 (1998) 107.
[24] P.J. Linstrom, W.G. Mallard, NIST Chemistry WebBook, National Institute of Standard and Technology, Gaithersturg, MD, 20899. (2010) Available from: <http://webbook.nist.gov/chemistry/>.
[25] R.D. Bowen, A. Maccoll, Org. Mass Spectrom. 19 (1984) 379.
[26] W.J. Lambdin, B.L. Tuffly, V.A. Yarborough, Appl. Spectrosc. 13 (1959) 71.
[27] E.T.M. Selim, A.I. Helal, Indian J. Pure Appl. Phys. 19 (1981) 977.
[28] J.D. Shao, T. Baer, D.K. Lewis, J. Phys. Chem. 92 (1988) 5123.
[29] V.K. Potapov, V.V. Sorokin, Khim. Vys. Energ. 6 (1972) 387.
[30] D. Harnish, J.L. Holmes, F.P. Lossing, A.A. Mommers, A. Maccoll, M.N. Mruzek, Org. Mass Spectrom. 25 (1990) 381.
[31] R.F. Sawyer, Proc. Combust. Inst. 24 (1992) 1423.
[32] M.J. Papachristos, J. Swithenbank, G.H. Priestman, S. Stournas, P. Polysis, E. Lois, J. Inst. Energy 64 (1991) 113.
[33] A. Arce, H. Rodriguez, A. Soto, Green Chem. 9 (2007) 247.
[34] M. Vosahlikova, K. Demnerova, J. Pazlarova, Chem. Listy 102 (2008) 102.
[35] F.P. Lossing, J. Am. Chem. Soc. 99 (1977) 7526.
[36] M. Klessinger, P. Asmus, U. Kraatz, Tetrahedron 31 (1975) 517.
[37] J.C. Person, P.P. Nicole, Argonne National Laboratory Radiological Physics Division Annual Report, July 1967–June 1968, ANL 7489, p. 105.
[38] A.A. Mommers, P.C. Burgers, J.L. Holmes, J.K. Terlouw, Org. Mass Spectrom. 19 (1984) 7.
[39] C.H. DePuy, S.R. Kass, G.P. Bean, J. Org. Chem. 53 (1988) 4427.